

Frontiers of Experimental Condensed Matter Physics

■ Part C, Atomic scale measurements: Scanned Probe Microscopies

■ First Lecture

- Principles of probe microscopes
 - Tunnelling microscopy
 - Force microscopy
- Tunnelling microscopy
 - Basic theory
 - Morphology and spectroscopy
 - Case study: Si(111)

■ Second lecture

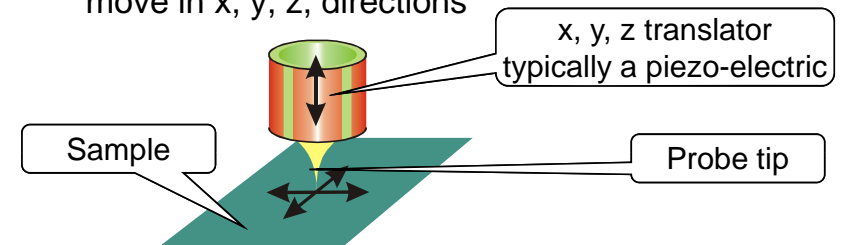
- Force microscopy
 - Atomic forces
 - Contact and non-contact methods
- Atom manipulation
 - Moving atoms and molecules
 - Dissociating and reacting atoms and molecules

1

Principles

■ Local probes

- Spatial resolution comes from a confined probe, which is usually a sharp point. Generally able to move in x, y, z, directions

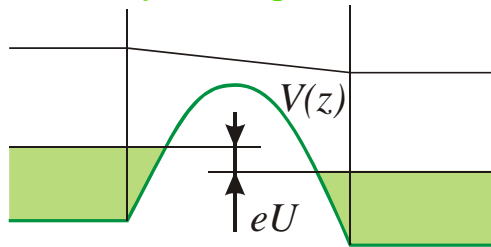


- Classic example is the Tunnelling microscopy, STM, where microscopy with electrons at atomic resolution is achieved by directing electrons through a single atom – the finest possible probe.
- There are many variants on the method, eg:
 - Scanning near-field optical microscopy
 - Magnetic force microscopy
 - Scanning capacitance microscopy.
- We concentrate on two of the most common and important:
 - Scanning tunnelling microscopy (STM)
 - Atomic force microscopy (AFM)

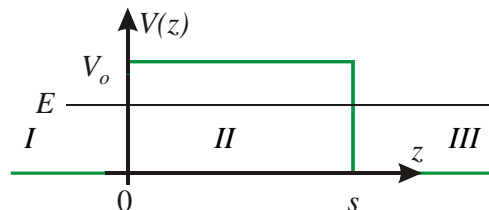
2

Tunnelling microscope

1-D barrier separating two metals



- In general there is a voltage (bias), U , between the metals, and the potential, $V(z)$, includes the image potential.
- The simplest model is to replace set the bias to zero and make the barrier rectangular (one of the first problems encountered in Quantum Mechanics)



$$\psi_I = \exp(ikz) + A \exp(-ikz) \quad \psi_{III} = D \exp(ikz)$$

$$\psi_{II} = B \exp(-\chi z) + C \exp(\chi z)$$

$$\chi^2 = 2m(V_0 - E)/\hbar^2$$

$$k^2 = 2mE/\hbar^2$$

3

- Matching ψ and $d\psi/dx$ at boundaries gives the transmitted current $T=j_{III}/j_I=|D|^2$.

$$T = 1 / \left(1 + \frac{(k^2 + \chi^2)^2}{4k^2 \chi^2} \sinh^2(\chi s) \right)$$

- In the limit of a strongly attenuating barrier

$$T \propto \exp(-2\chi s) \quad \text{A}$$

- The behaviour is typical in that strong exponential dependence with a dependence on $(V_0 - E)^{1/2}$ arises independently of the exact shape of the barrier.
- Orders of magnitude: If $s = 5\text{\AA}$, and the effective barrier height is 4eV , $T \approx 10^{-5}$. Increasing s by 1\AA reduces T by an order of magnitude.

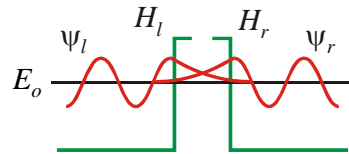
Time-dependent approach

- Before looking at the 3-D problem, we consider an alternative approach to the simple 1-D problem. The aim is to exploit the small transmission probability and seek a perturbation treatment.
- First solve the separate problems of the left barrier (in the absence of the right) and the right barrier in the absence of the left.

See: Wiesendanger, Ch1.11

4

Transfer Hamiltonian method



- Solutions are:

$$\psi_l = a \exp(-\chi z); \quad z \geq 0$$

$$\psi_r = b \exp(\chi z); \quad z \leq 0$$

and the current is given by Fermi's Golden Rule

$$j_t = \frac{2\pi e}{\hbar} |\langle \psi_r | H_T | \psi_l \rangle|^2 \frac{dN}{dE_r}$$

$H - E_0$

Density of final states

- The result is identical to eq. A, p. 4. Note, it is straightforward to add a sample bias (see below) as we only need the solution in the vacuum region.

Tunnelling in 3-D. (Bardeen, *Phys. Rev. Lett.* 6 (1961) 57)

- Generalising the above method

$$I = \frac{2\pi e}{\hbar} \sum_{\mu, \nu} \{ f(E_\mu) [1 - f(E_\nu + eU)] - f(E_\nu + eU) [1 - f(E_\mu)] \} |M_{\mu\nu}|^2 \delta(E_\nu - E_\mu)$$

- $f(E)$ is the Fermi function and tunnelling both ways is included.

5

- Bardeen argued that the tunneling matrix element is given by

$$M_{\mu\nu} = \frac{-\hbar^2}{2m} \int dS \cdot (\psi_\mu^* \nabla \psi_\nu - \psi_\nu \nabla \psi_\mu^*)$$

where the integral is over any surface lying entirely in the vacuum region. To calculate the expression in parentheses (current density) we need a model of the tip.

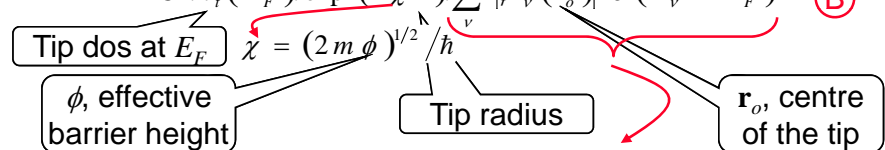
- Tersoff and Hamann (*Phys. Rev. B* 31, (1985) 805) were first to apply the method to STM. They modelled the tip as a sphere (*s*-wave only, higher *l*-values are neglected).

- At low temperature and low bias,

$$I = \frac{2\pi e^2 U}{\hbar} \sum_{\mu, \nu} |M_{\mu\nu}|^2 \delta(E_\nu - E_F) \delta(E_\mu - E_F)$$

- Using the *s*-wave approximation, they obtained

$$I \propto U \cdot n_t(E_F) \cdot \exp(2\chi R) \cdot \sum |\psi_\nu(\mathbf{r}_o)|^2 \delta(E_\nu - E_F) \quad \textcircled{B}$$



Local density of states (LDOS) of the sample states at the Fermi energy, calculated at the position of the tip centre.

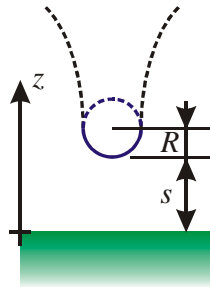
6

z-dependence of the tunnelling

- In the vacuum, the sample wavefunction decays exponentially

$$\psi_v \propto \exp(-\chi z)$$

- Hence, the amplitude at the centre of the tip is $|\psi_v|^2 \propto \exp(-2\chi(s+R))$ and the current is $I \propto \exp(-2\chi s)$.

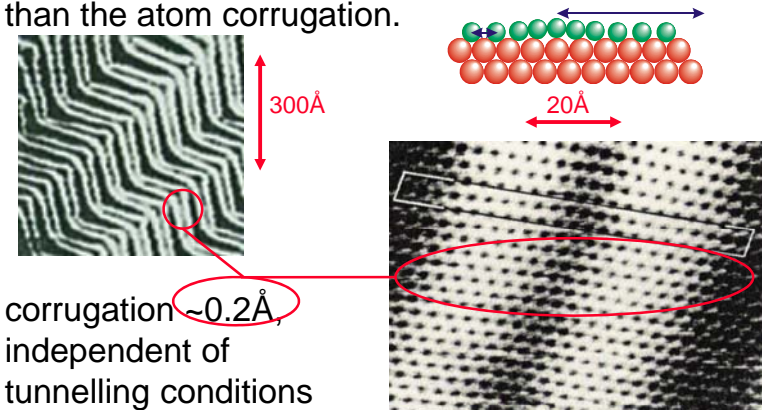


- The simple theory gives us two key results:
 - The current decreases exponentially with z .
 - The tunnelling current depends on the sample, LDOS measured at the tip site.
- The two results are the origin of, respectively,
 - Atomic resolution. (Recall, the decay rate with z means that a 1% change in current corresponds to a z -displacement of $\sim 0.02\text{\AA}$).
 - Spectroscopy (STS). The ability to map electronic states.
- Both ideas need further exploration.....

7

Lateral resolution

- What about the lateral resolution?
- A corrugation decays rapidly into the vacuum region. Tersoff and Hamman show that, for a lateral variation of period, a , the corrugation Δ is $\Delta \propto \exp(-G^2 z/4\chi)$, where $G = 2\pi/a$. Only the lowest Fourier components will be seen.
- Example: Au(111) has 23 surface atoms for 22 bulk atoms, leading to a misfit and a long range corrugation (approximately as sketched). The long range periodicity is much easier to observe than the atom corrugation.

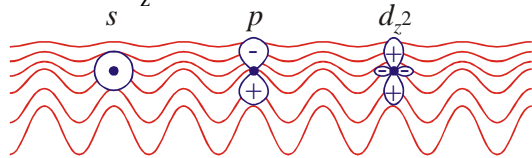


- corrugation $\sim 0.2\text{\AA}$, independent of tunnelling conditions
- atomic corrugation is much smaller and only observable under favourable conditions

8

Tip states

- On the basis of s-wave, tip states, one would not expect to see atomic corrugation on close-packed metal surfaces.
- It follows that lateral resolution depends on the dominant tip orbitals. The sketch shows s , p and d orbitals embedded in a corrugated charge. Clearly the lateral averaging is more for the s -state and least for the d_{z^2} -state.



(See Chen, *Phys Rev* **B42** (1990) 8841, for a quantitative treatment).

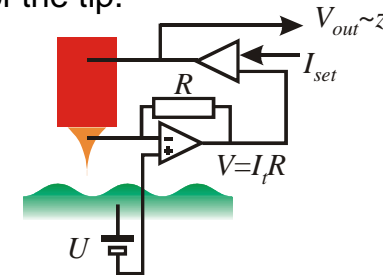
- The fact that the resolution depends on the electronic state at the tip may explain why tips with d -states are the most common in practice (typical materials are Tungsten or Pt/Ir alloy).
- Modern simulations rely on *ab-initio* calculations of the sample states and a quantitative treatment of the tunnelling.

9

Constant current images

■ Imaging at constant current:

- The usual mode of operation is for the tip height to be adjusted to maintain the current constant. The measured current is fed-back to the z-piezo control and (if the piezo actuator is linear) the voltage driving the piezo is proportional to the height of the tip.



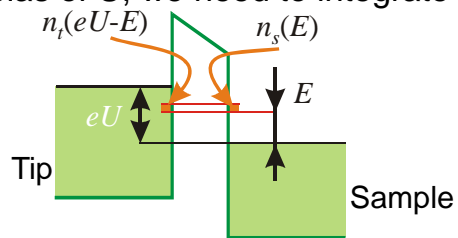
- In constant current mode, at small bias voltage, the height, z , is a contour of constant density of states, at E_F . Thus, there are two main components to the image:
 - sample morphology.
 - sample density of states.
- It can be difficult to separate the two components, in the image without careful consideration.

10

Spectroscopy

■ Scanning tunnelling spectroscopy

- We need to generalise the basic, low bias formula for the tunnelling current Eq. (B), on p 6.
- At a bias of U , we need to integrate over E



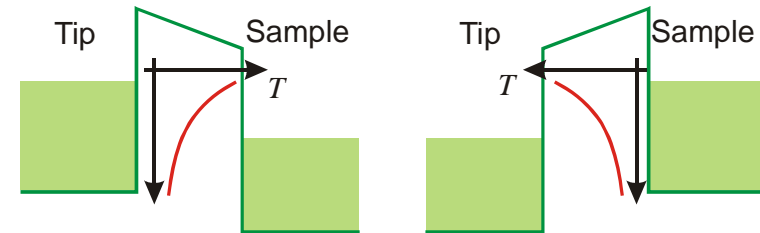
(energies of tip and sample measured wrt their respective E_F). The total current is

$$I \propto \int_0^{eU} n_t(eU - E) n_s(E) T(E, eU) dE$$

Tip dos Sample dos Transmission coeff.

- The formula suggests that the tip and sample states contribute equally to the current. In fact it is the variation of the empty state density that is most important, see below...

- In general, the largest contribution to the current is determined by the transmission coefficient. States with the highest energy see the smallest effective barrier and give the highest transmission.

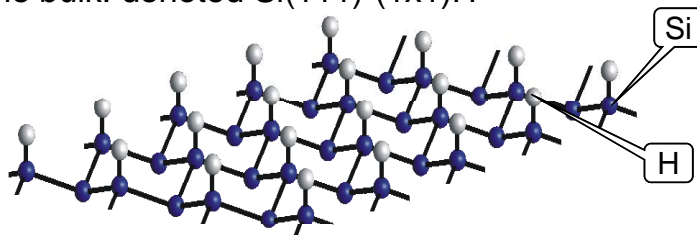


- Thus, in the left figure (Tip biased negatively) the current is predominantly due to electrons at E_F of the tip. The strongest changes in current are due to changes in the sample dos.
- Similarly, in the right figure (Tip biased positively) the current is predominantly due to electrons at E_F of the sample, and the strongest changes in current are due to changes in the tip dos.

Case study Si(111)

■ Si(111) –(7x7)

- Atoms at the silicon (111) surface re-arrange to form a 7x7 surface unit cell. For many years its remained an unsolved structural problem. Early STM measurements helped to elucidate the structure and marked the breakthrough of the STM method
- Silicon atoms bond tetrahedrally and when cut to expose the 111 surface each atom has a single bond directed out of the surface. When that bond is saturated (for example by adsorbing hydrogen), the surface structure has the same periodicity as the bulk: denoted Si(111)-(1x1)H



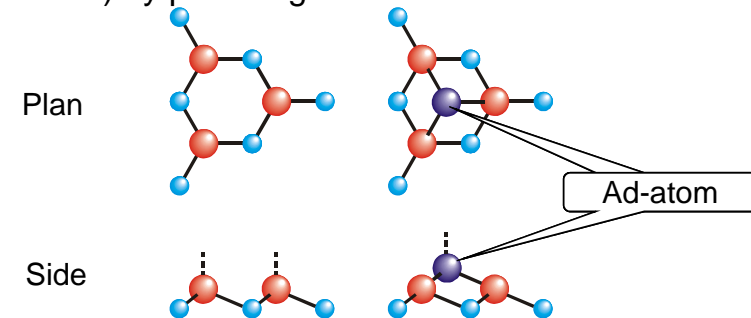
- When the hydrogen is absent the bonds are unsaturated and the surface reconstructs to lower its energy

Ref: Wiesendanger pp. 293

13

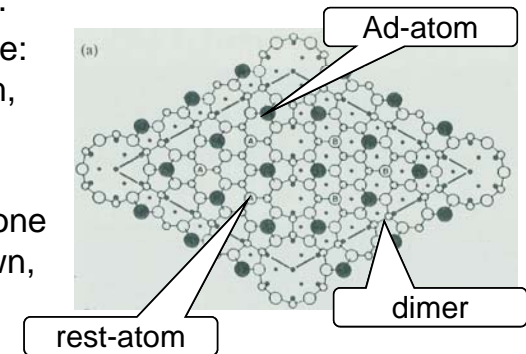
(7x7) reconstruction

- The number of dangling bonds is reduced (from 49 to 19) by providing ad-atoms



Note there is some lattice distortion necessary to accommodate the ad-atoms. There are also other aspects of the reconstruction that relieves the lattice strain (a stacking fault and dimer formation in lower layers).

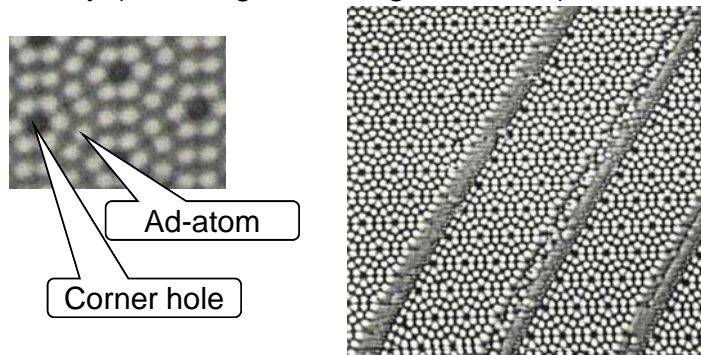
- Hence the name: Dimer, Ad-atom, Stacking fault (DAS) model.
- A plan view of one unit cell is shown, right.



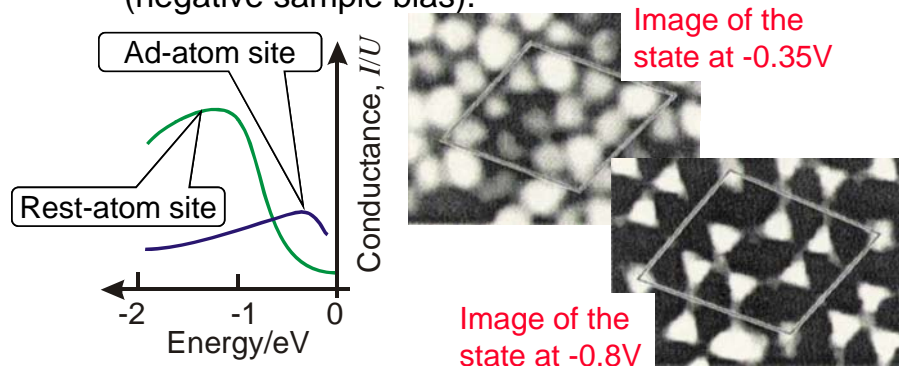
14

Si(111)- Images

- Constant current images (tunnelling into empty sample states) show the positions of the ad-atoms clearly (left image is a single unit cell).



- Spectroscopy: data shown for occupied states (negative sample bias).



Ref: Hamers et al: Phys Rev Lett 56 (1986) 1972
Ann Rev Phys Chem 40 (1989) 531

15

■ Notes:

- Images are remarkable for their clarity and the ease with which features can be attributed to specific atoms (Si(111) is almost unique in this regard).
- Empty state images (top half of previous page) are dominated by the ad-atoms
- Conductance curves taken at different lateral positions show maxima that can be attributed to localised, surface states.
- Filled state images of these states (bottom half of previous page) show ad-atoms at low bias voltages and the rest-atoms at higher bias voltages.
- The ability to image electronic states is a unique attribute of the STM method.
- Note the asymmetry in the occupied-state image at -0.35V, which is due to the stacking fault. It follows that the underlying layers play some role in the tunnelling.

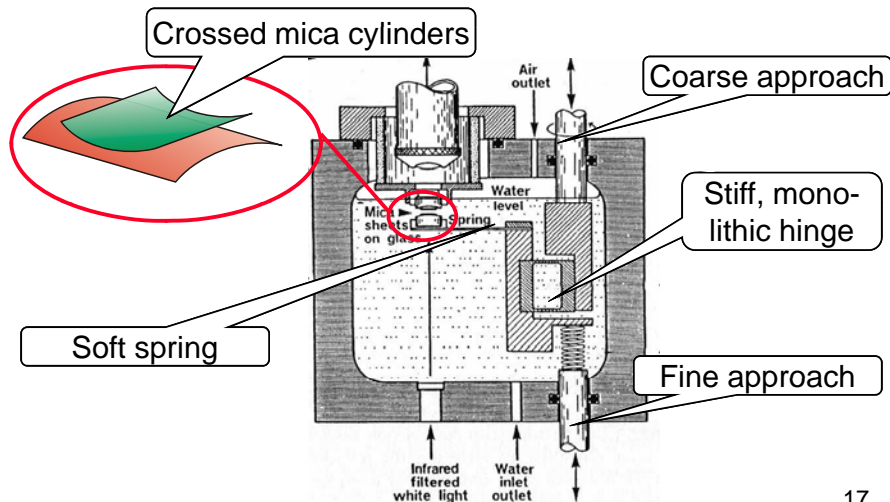
16

Force Microscopy

- Tunnelling microscopy can only be used on metallic samples. Force microscopy is applicable to conducting and non-conducting samples. It uses a fine probe and measures the force between sample and probe.

Historical note:

- Some of the methods derive from pioneering experiments done at the Cavendish by Tabor and others (especially Israelichvili); see museum.
- Their interest was in determining surfaces forces

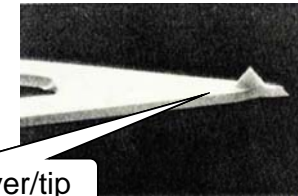


17

SFM/AFM

Scanning Force Microscopy (SFM):

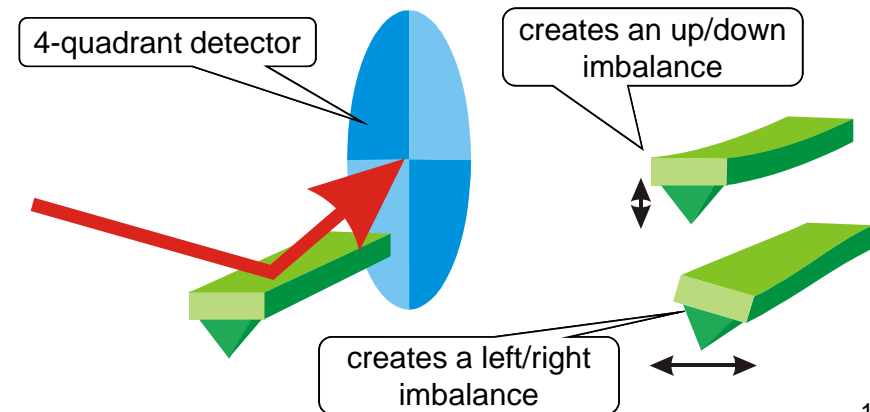
- also called Atomic Force Microscopy (AFM)
- The method derives its spatial resolution from a sharp probe mounted on a sprung cantilever. These are usually micro-fabricated with integrated tips.



SiO₂ cantilever/tip

40μm

- Cantilever deflection is often determined by reflection of a laser beam. A 4-quadrant detector allows measurement of both vertical and torsional motion of the cantilever



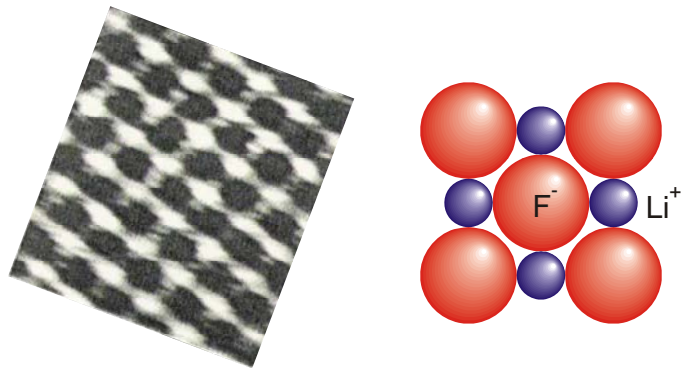
18

Imaging in contact mode

- The instrument can be used in either contact mode, where the tip is in permanent contact with the sample, or in non-contact mode.

■ Contact mode

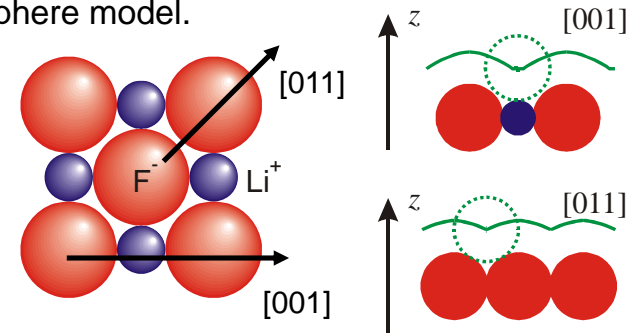
- Constant force imaging: the cantilever is manipulated by piezo drives to maintain a constant cantilever deflection. The forces are repulsive and, under favourable conditions, atomic resolution is possible.
- Example: LiF(100), the protrusions seen are ascribed to the larger F^- ion.



Meyer et al. J. Vac. Sci. Technol. **B9** (1991)1329

19

- The ionic radius of Li^+ (0.68\AA) is much less than F^- (1.33\AA) and is invisible. The corrugation was originally interpreted in terms of a rigid, hard-sphere model.

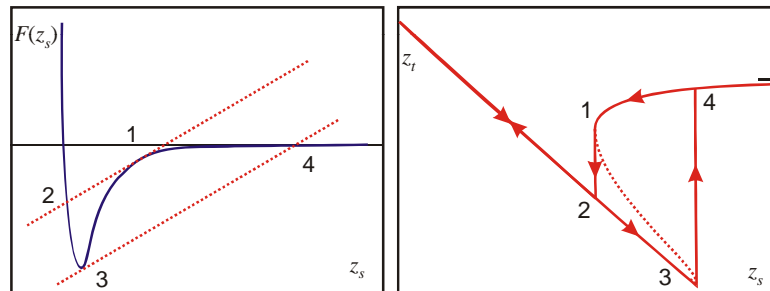


- The forces used to generate images are typically 10^{-8} - 10^{-7} N. With a single atom tip, such forces will cause deformations in the sample (and/or tip).
- Some early images (~1990) showed atomic resolution with giant corrugations. These are now believed to be artifacts. A full explanation of the images remains to be achieved.
- Accurate modelling of the images requires the mechanical properties of the tip and sample to be included. Such simulations are now possible (see later)

20

Force spectroscopy

- Measurements of cantilever displacement versus distance can, in principle, lead to direct measurements of the surface forces
- If z_t is the cantilever deflection and z_s the position of the sample, then the behaviour follows from the force-distance relationship, $F(z_s)$.
 - As the sample is moved towards the tip, the attractive forces cause the cantilever to deflect towards the sample and z_t decreases.
 - Point 1: Eventually the slope of the force-distance curve exceeds the spring constant of the cantilever and the tip snaps into contact with the surface, at point 2.
 - Further motion of the sample causes the cantilever to bend outwards and repulsive forces dominate.



21

■ Hysteresis

- Reversing the motion gives a different curve:
 - Point 3: the tip remains in contact with the surface, initially with repulsive forces then through attractive forces until the maximum adhesive force is reached (i.e. when the force gradient equals the cantilever spring-constant)
 - Point 4: at this point the cantilever springs backwards and contact is lost.
- Real tip-surface interactions are more complex.
- For example:
 - the forces on a sharp tip can exceed the elastic limit.
 - in air, water condensation near the tip may add capillary forces and give instability. When fully immersed the capillary forces are absent and smaller tip-sample interactions can be probed.
- See Nature news and views feature (Yazdani and Lieber, Nature 401 (1999) 227) for recent applications.

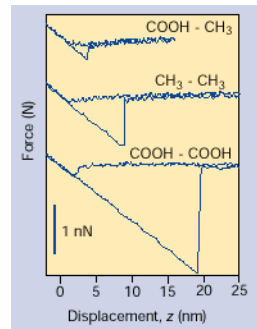
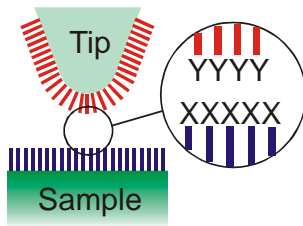
22

Forces in Chemistry and Biology

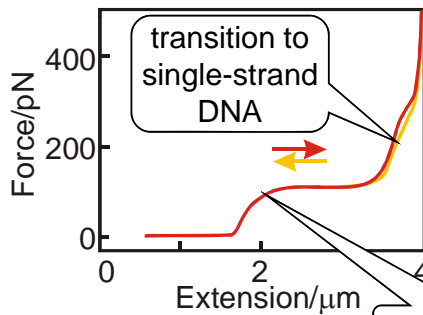
Examples

Adhesion forces in Chemistry:

- take a tip modified with a functional monolayer having a known termination (Y) and the sample with a different termination (X).
- Force spectroscopy allows a direct measurement of the X-Y adhesion.



Mechanical properties of single bio-molecules:



Attaching one end of the molecule to the tip and the other to the sample, allows measurement of the mechanical properties of single molecules eg. DNA

(Biophys. J. 78 (2000) 1997) 23

Non-contact AFM

- In the contact-mode, experiments are predominantly sensitive to repulsive forces and they are sensed by quasi-static deflection of the cantilever.
- In the non-contact mode, the tip-surface separation is greater and the forces smaller. The cantilever deflection is too small to measure statically.
- Instead, it is set to vibrate at its resonant frequency, ω_o , and changes in ω_o are used to create the image. The main effect is to change the spring constant due to the local force-gradient, $F' = \partial F_z / \partial z$.
- An attractive force, $F' > 0$, softens the spring constant $c_{eff} = c - F'$

$$\omega = \left(\frac{c_{eff}}{m} \right)^{1/2} = \left(\frac{c}{m} \right)^{1/2} \left(1 - \frac{F'}{c} \right)^{1/2}$$
- The change in frequency is a direct measure of the force-gradient

$$\Delta \omega = \omega - \omega_o \approx -F' / 2c$$
 - the frequency decreases for an attractive interaction

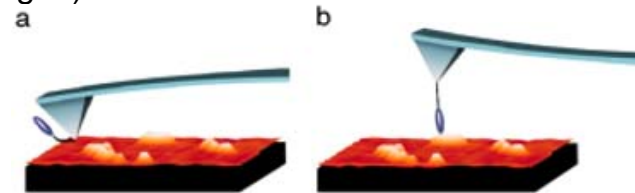
- Since frequency shifts can be determined very accurately, the non-contact mode offers superior sensitivity in most cases.
- Maps of frequency shift can be obtained at the same time as the usual topographic images, giving two complementary views of the sample.
- Typical operating conditions are:
 - oscillation amplitude 1-5 nm.
 - oscillation frequency ~10kHz
 - oscillation Q-value:
 - In vacuo $Q \sim 10^4$
 - in air $Q \sim 100$
 - in liquid $Q \sim 1$

■ **Example:** Single-molecule recognition.

- The use of a functionalised tip to identify specific bio-molecules. (Stroh et al. PNAS **101** (2004) 12503)
- Non-contact, AFM is widely used to study biological systems; however, topographic images lack clear contrast. DNA can be identified by its thread-like appearance but different protein components look similar.

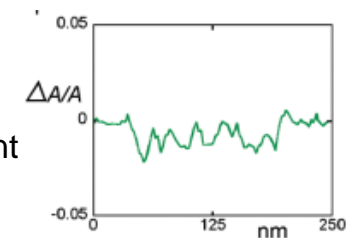
25

- By tethering an antibody to the tip, a specific contrast mechanism occurs.
- When there is no antigen, the tip operates normally (fig. a); However, when the tip approaches an antigen, the antibody binds to a specific site and the cantilever motion is disturbed (fig. b).



Specifically, the oscillation amplitude dips slightly, by an amount ΔA , before being re-established as the instrument continues to scan. Thus, a map of ΔA , as the tip scans, identifies the location of antigen sites.

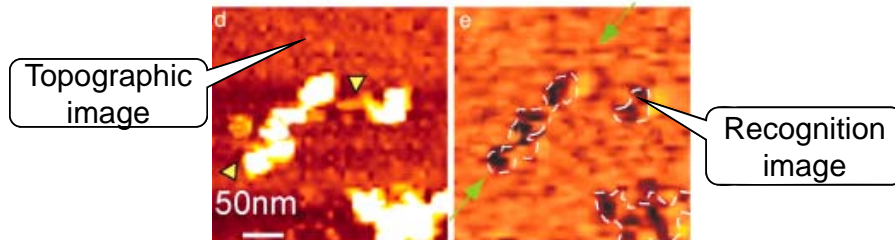
- Typical variation of $\Delta A/A$ during a scan are shown in the figure (right) and amount to changes of ~2%. Clear dips in ΔA are visible.



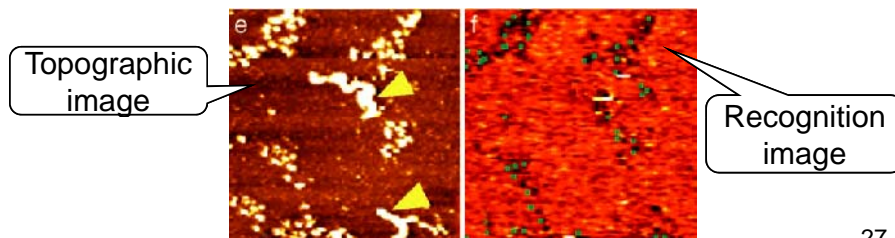
26

Atom Manipulation

- A conventional topographic image taken alongside a ΔA map gives the following:



- Topographic image (left): nucleosomal arrays are the light patches, with a “height” of ~5nm.
- The recognition image (right) shows darker patches that correspond to specific antibody-antigen recognition events.
- Specificity is demonstrated by a mixture of proteins (below). Green dots (right), showing recognition, do not occur for proteins without the antigen (shown by yellow arrows in the left image)



27

■ Nanotechnology

- Scanned probe methods (STM, AFM) have been used to manipulate samples as well as observe them.
- A key breakthrough was the controlled manipulation of single atoms (see Stroschio and Eigler, Science 254 (1991) 1319, and references therein.). Several processes have been identified:

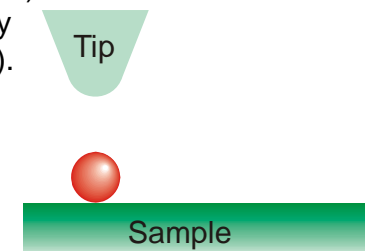
■ Soft manipulation Lateral motion of Xe atoms.

- Through a combination of tip motion and changes in tunnelling current:

☞ Position tip (~1 nA, 10mV) and move towards atom by increasing current (~16nA).

☞ Move tip laterally to pre-determined destination.

☞ Retract tip by reducing current to original value.



28

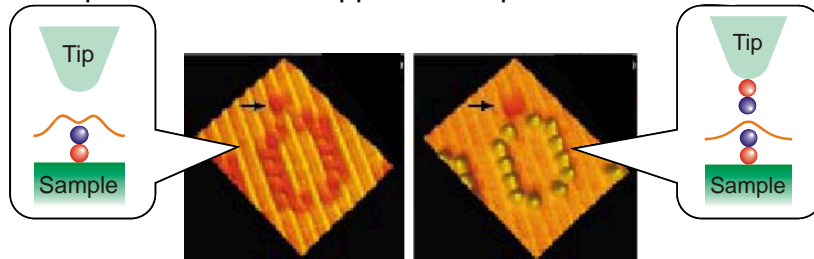
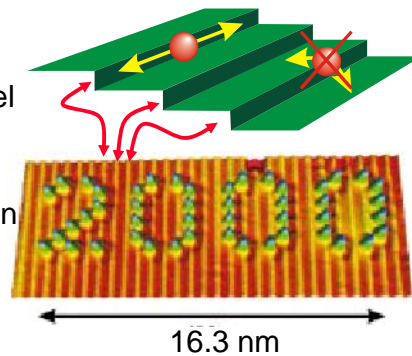
Molecules

- Similar behaviour reported for some molecules, where surface features, such as steps, affect the motion.

eg: for CO on stepped copper (Cu(211)), manipulation is easy parallel to steps but difficult in the perpendicular direction.

The number "2000" written in CO molecules (See Hla, Meyer Rieder CHEM PHYSICHEM 2001, 2, 361)

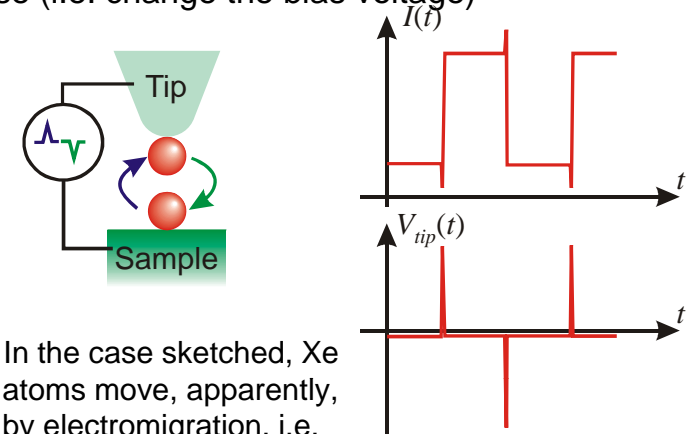
Note regarding the image: The CO adsorbates are seen as a protrusion when the tip has a CO molecule attached. Without a "CO-functionalised" tip the adsorbates appear as depressions.



29

Vertical manipulation

- The last images raise the question of how to get CO molecules onto the tip. This is the topic of vertical manipulation.
- The processes are complex and not well understood. The procedure is to place the tip above the atom/molecule and apply a current pulse (i.e. change the bias voltage)



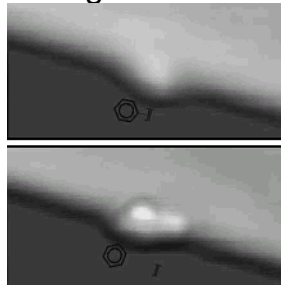
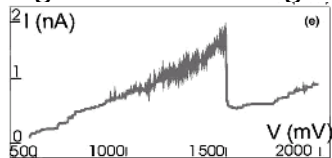
- In the case sketched, Xe atoms move, apparently, by electromigration. i.e. the flux of electron drives the transition.
- Note, the $I(t)$ curve shows that the conductance of the junction has changed. The change is, therefore, indicative of the transition having taken place.

30

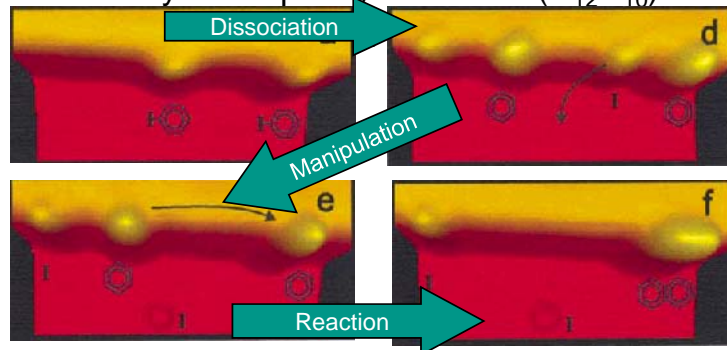
Dissociation and assembly

Atomic-scale reactions

- A further manipulation process is dissociation (See: Chem Phys Lett 370 (2003) 431). In dissociation of iodobenzene C_6H_5I by the tunnelling current, the tip bias is changed continuously. The signature of dissociation is seen as a sudden change in current (left figure). “Before” and “after” images are shown right.



- Complete reactions have been performed: Dissociation of 2 iodobenzenes and assembly of a biphenyl molecule ($C_{12}H_{10}$)



Ref: PRL 85 (2000) 2777

31